

# Alkyne-Stabilized Ruthenium Nanoparticles: Manipulation of Intraparticle Charge Delocalization by Nanoparticle Charge States\*\*

Xiongwu Kang, Nathaniel B. Zuckerman, Joseph P. Konopelski, and Shaowei Chen\*

Monolayer-protected transition metal nanoparticles<sup>[1–4]</sup> are a unique family of functional nanomaterials in which the properties of the materials can be readily manipulated not only by the chemical nature of the metal cores and the organic protecting ligands, but also the metal–ligand interfacial bonding interactions. The latter is largely motivated by recent progress in nanoparticle passivation by metal–carbon covalent bonds, where intraparticle charge delocalization may occur as a result of the strong metal–carbon interfacial bonding interactions, in sharp contrast to nanoparticles that are functionalized by mercapto derivatives. For instance, when ferrocene moieties are bound onto a ruthenium nanoparticle surface by ruthenium–carbene  $\pi$  bonds, effective intervalence transfer occurs between the ferrocenyl metal centers at mixed valence, as manifested in electrochemical and near-infrared (NIR) spectroscopic measurements and density functional calculations.<sup>[5,6]</sup> Furthermore, when fluorophores are attached onto the nanoparticle surface by the same conjugated linkage, novel emission characteristics emerge that are consistent with those of dimeric derivatives with a conjugated spacer.<sup>[7,8]</sup> In a more recent study,<sup>[9]</sup> effective intraparticle charge delocalization was also observed with ruthenium nanoparticles passivated by alkynyl fragments. This result was ascribed to the unique interfacial bonding interactions (Ru–C $\equiv$ ) formed by ruthenium and sp-hybridized carbon atoms of the ligands.

In these studies, the nanoparticle metal cores serve as the conducting media to facilitate charge transfer between the functional moieties covalently bound onto the nanoparticle surface. Therefore it is anticipated that the extent of intraparticle conjugation may be readily controlled by the nanoparticle charge state, which is the primary motivation of the present study. Experimentally, by exploiting the molecular capacitor characters of Ru–C $\equiv$  nanoparticles, the charge states of the nanoparticles were varied by simple chemical reduction or oxidation. The impacts of the nanoparticle charge states on the particle optical and electronic properties were then carefully examined by FTIR spectroscopy, X-ray

photoelectron spectroscopy (XPS), and photoluminescence measurements, and compared to those of the as-prepared nanoparticles.

The synthetic procedure for the preparation of ruthenium nanoparticles passivated by 1-octynyl fragments (Ru-OC) has been detailed previously.<sup>[9]</sup> TEM measurements showed that the nanoparticles exhibited an average core diameter of  $(2.55 \pm 0.15)$  nm. The nanoparticle charge states were then varied by chemical redox reactions.<sup>[10]</sup> Specifically, to render the nanoparticles negatively charged, in a typical reaction, 5 mg of Ru-OC nanoparticles were dissolved in dichloromethane (1 mL); a freshly prepared water solution of NaBH<sub>4</sub> (1 mL, 5 mg mL<sup>-1</sup>) was then added. The mixture was stirred for 30 min and then water was removed. The resulting nanoparticles exhibited negative net charges and were denoted as Ru-OC<sub>Red</sub>. Positively charged nanoparticles were prepared in a similar fashion by mixing the nanoparticle solution with an aqueous solution of saturated Ce(SO<sub>4</sub>)<sub>2</sub> for 30 min. The resulting nanoparticles were denoted as Ru-OC<sub>Ox</sub>.

Transition metal nanoparticles passivated with a low-dielectric organic protecting layer have long been known to act as nanoscale molecular capacitors. In fact, based on a concentric structural model,<sup>[11]</sup> the nanoparticle capacitance ( $C_{MPC}$ ) can be estimated by  $C_{MPC} = 4\pi\epsilon_0\epsilon(r+d)\frac{r}{d}$ , where  $\epsilon_0$  is the vacuum permittivity,  $\epsilon$  is the effective dielectric constant of the organic protecting layer,  $r$  is the radius of the metal core, and  $d$  is the length of the organic protecting ligand. For the octyne-passivated ruthenium (Ru-OC) nanoparticles,  $r = 1.275$  nm,  $d = 0.848$  nm (estimated by Hyperchem), and  $\epsilon = 2.6$ .<sup>[12]</sup> Thus, the nanoparticle capacitance can be estimated to be about 0.92 aF. To quantify the change of the nanoparticle charge state after reduction or oxidation, we measured the open circuit potentials of the nanoparticles electrochemically. It was found that the as-prepared Ru-OC nanoparticles exhibited an open circuit potential of +0.140 V (versus Ag/AgCl). After reduction by NaBH<sub>4</sub>, it decreased to +0.024 V, whereas after oxidation by ceric sulfate, it increased to +0.250 V. This result indicated that the reduced nanoparticles (Ru-OC<sub>Red</sub>) exhibited an average charging of 0.67 electrons per nanoparticle, whereas the oxidized nanoparticles (Ru-OC<sub>Ox</sub>) were formed by an average discharging of 0.63 electrons per nanoparticle.

Interestingly, despite these subtle changes of nanoparticle charge states, rather drastic impacts were observed on the nanoparticle optoelectronic properties. Figure 1 depicts the FTIR spectra of the nanoparticles before and after reduction or oxidation. For the as-prepared Ru-OC nanoparticles, the C $\equiv$ C stretching band appeared at 1965 cm<sup>-1</sup> (inset). In comparison to octyne monomers, for which the C $\equiv$ C stretch-

[\*] X. W. Kang, N. B. Zuckerman, Prof. J. P. Konopelski, Prof. S. W. Chen  
Department of Chemistry and Biochemistry, University of California  
1156 High Street, Santa Cruz, CA 95064 (USA)  
Fax: (+1) 831-459-2935  
E-mail: shaowei@ucsc.edu  
Homepage: <http://chemistry.ucsc.edu/~schen>

[\*\*] This work was supported by grants from the National Science Foundation (CHE-0718170 and CHE-0832605). XPS data were acquired at the Molecular Foundry, Lawrence Berkeley National Laboratory, which is supported by the US Department of Energy.

Supporting information for this article is available on the WWW under <http://dx.doi.org/10.1002/anie.201004967>.

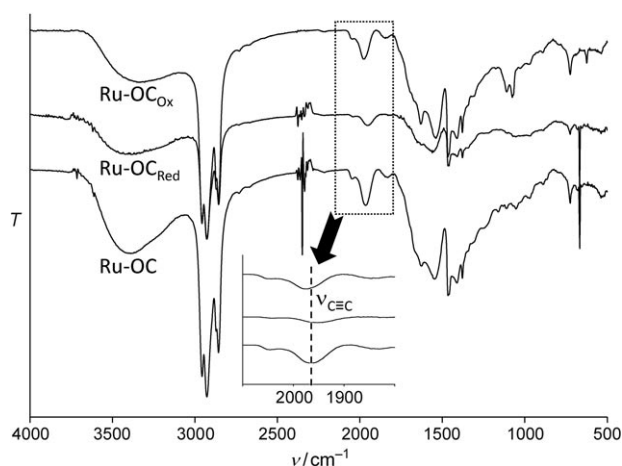


**Figure 1.** Transmittance IR spectra of Ru-OC nanoparticles before and after reduction and oxidation. Inset: magnification of the portions enclosed by the dotted box; the C≡C vibrational stretch is highlighted by the dashed line.

ing bands was observed at  $2116\text{ cm}^{-1}$ , this substantial red-shift is ascribed to the bonding coordination of the acetylene moieties of the octyne ligands to the ruthenium metal cores,<sup>[9]</sup> where  $\pi$  bonds were formed by the overlap between the  $d_{\pi}$  orbital or the  $p_{\pi}d_{\pi}$  hybrid of the metal and the  $\pi^*$  orbital of the octynyl sp carbon atoms,<sup>[13,14]</sup> leading to the decrease of the C≡C bonding order.

After reduction by  $\text{NaBH}_4$  however, the C≡C band red-shifted further to  $1953\text{ cm}^{-1}$ , whereas oxidation by ceric sulfate led to an apparent blue-shift to  $1977\text{ cm}^{-1}$ . The former suggests a further decrease of the C≡C bonding order, whereas in the latter, the bonding order was enhanced somewhat. Previously we showed that because of the strong Ru–C≡ interfacial bonding interactions, the particle-bound acetylene moieties behaved analogously to diacetylene derivatives,  $-\text{C}=\text{C}-\text{C}=\text{C}-$ .<sup>[9]</sup> Therefore, charging of extra electrons (by chemical reduction) into the nanoparticle cores led to an electron-rich metal core, where back-bonding of metal electrons to the  $\pi^*$  orbital of the octyne ligands was favored. In other words, the enhanced intraparticle charge delocalization further decreased the bonding order of the C≡C moieties and hence produced a more pronounced red-shift of the C≡C stretching band. In contrast, chemical oxidation (by ceric sulfate) led to depletion of electrons from the metal core, resulting in reduced back-bonding of the metal d orbitals to the  $\pi^*$  orbital of the sp-hybridized carbon of the octyne ligands. Because of this diminishment of intraparticle extended conjugation, the C≡C bonding order increased (that is, the functional moieties became more independent) and thus a blue-shift of the stretching band energy was observed.<sup>[15]</sup>

The variation of the C≡C bonding order with nanoparticle charge state was also manifested in XPS measurements. We focused on the C1s binding energy, which consists of contributions from both sp and  $\text{sp}^3$  carbon atoms. By peak deconvolution (Supporting Information, Figures S1, S2), and regardless of the nanoparticle charge state, the binding energies of the  $\text{sp}^3$  carbon atoms were all identified at

$285.2\text{ eV}$ , in agreement with earlier reports.<sup>[16,17]</sup> This result signifies minimal impacts of the metal–ligand interfacial bonding interactions on the electronic structure of the alkyl components. However, the C1s binding energy of the sp carbons exhibited a clear variation with the nanoparticle charge state (Figure 2). For the as-prepared Ru-OC nano-

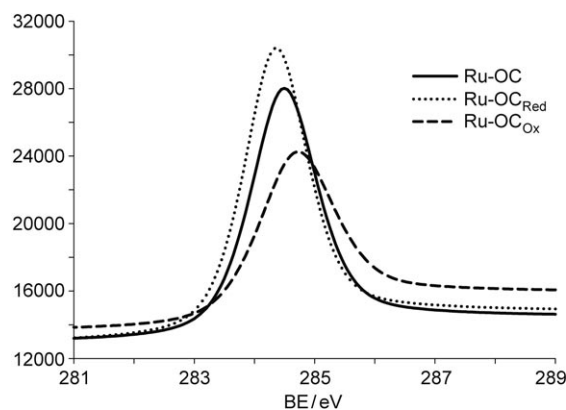


**Figure 2.** XPS spectra of sp-hybridized carbon atoms (C1s electrons) of Ru-OC nanoparticles before and after reduction and oxidation. BE = binding energy. The spectra were obtained by deconvolution of the original data, for which the contributions of  $\text{sp}^3$  carbon atoms were removed (see Supporting Information, Figures S1, S2).

particles, the binding energy of the sp carbon atoms appeared at  $284.49\text{ eV}$ , whereas after reduction and oxidation, the binding energy shifted to  $284.36\text{ eV}$  and  $284.75\text{ eV}$ , respectively. That is, the C1s binding energy of the sp-hybridized carbons decreases in the order of  $\text{Ru-OC}_{\text{Ox}} > \text{Ru-OC} > \text{Ru-OC}_{\text{Red}}$ , in agreement with the electron accepting (donating) characteristics in the Ru-OC<sub>Ox</sub> (Ru-OC<sub>Red</sub>) nanoparticles with respect to the as-prepared Ru-OC nanoparticles.<sup>[18]</sup> Nonetheless, despite the small variation, it can be seen that these binding energies are all very close to that of  $\text{sp}^2$ -hybridized carbon atoms observed with amorphous carbon or carbon nanotubes (ca.  $284.4\text{ eV}$ ),<sup>[17–21]</sup> suggesting extended conjugation within the nanoparticles as a result of the strong Ru–C≡ interfacial bonding interactions. This result is consistent with earlier observations that nanoparticle-bound ferrocene moieties exhibited intervalence charge transfer, as confirmed by voltammetric and near-infrared spectroscopic measurements.<sup>[9]</sup>

The binding energies of the  $\text{Ru}3d_{5/2}$  and  $\text{Ru}3d_{3/2}$  electrons in the nanoparticle cores also exhibited a similar variation with the nanoparticle charge states, which emerged as a broad peak centered at  $276.87\text{ eV}$ ,  $276.14\text{ eV}$ , and  $275.73\text{ eV}$  for the Ru-OC<sub>Ox</sub>, Ru-OC, and Ru-OC<sub>Red</sub> nanoparticles, respectively (Supporting Information, Figure S1). Therefore, adding further electrons into the nanoparticles (reduction) decreases the binding energies of the ruthenium d electrons, whereas discharging from the nanoparticles (oxidation) leads to an increase of the binding energy, a behavior that is commonly observed with ionic species in comparison to their elemental forms.<sup>[22]</sup> Furthermore, these binding energies are drastically smaller than those reported for metallic Ru ( $280.2\text{ eV}$  and

284.3 eV for the Ru3d<sub>5/2</sub> and Ru3d<sub>3/2</sub> electrons, respectively),<sup>[23,24]</sup> which again can be attributed to the extended intraparticle charge delocalization as a consequence of the strong Ru–C≡ interfacial bonding interactions.<sup>[9]</sup>

With such ready manipulation of the electronic structure of the metal cores and the organic protecting ligands, the nanoparticle luminescence also exhibited a sensitive variation with the nanoparticle charge state. Previously we reported that Ru-OC nanoparticles exhibited unique photoluminescence, which was accounted for by intraparticle charge delocalization as a result of the strong Ru–C≡ interfacial bonding interactions.<sup>[9]</sup> Therefore, the acetylene moieties bound onto the nanoparticle surface behaved equivalently to –C≡C–C≡C–. Figure 3 shows the excitation and emission

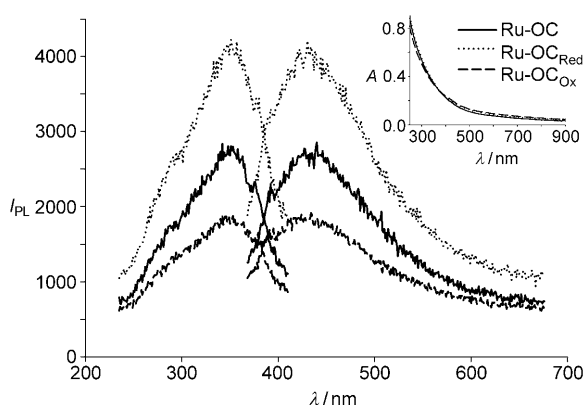


**Figure 3.** Excitation and emission spectra of Ru-OC nanoparticles in dichloromethane before and after reduction and oxidation.  $I_{\text{PL}}$  = photoluminescence intensity. Inset: corresponding UV/Vis absorption spectra of the three nanoparticles.

spectra of the Ru-OC nanoparticles before and after reduction or oxidation, where peak-shaped profiles are well-defined for all three nanoparticle samples. Table 1 summarizes the corresponding excitation ( $\lambda_{\text{ex}}$ ) and emission ( $\lambda_{\text{em}}$ )

**Table 1:** Summary of the excitation ( $\lambda_{\text{ex}}$ ) and emission ( $\lambda_{\text{em}}$ ) peak positions and emission intensities ( $I_{\text{em}}$ ) for the three nanoparticle samples, along with the absorbances ( $A$ ) at  $\lambda_{\text{ex}}$ .

	$\lambda_{\text{ex}}$ [nm]	$\lambda_{\text{em}}$ [nm]	$A$	$I_{\text{em}}$
Ru-OC <sub>Red</sub>	350	431	0.354	3972
Ru-OC	350	431	0.345	2674
Ru-OC <sub>Ox</sub>	347	428	0.345	1820

peak positions and emission intensities ( $I_{\text{em}}$ ), from which it can be seen that the as-prepared and reduced nanoparticles exhibited essentially identical  $\lambda_{\text{ex}}$  and  $\lambda_{\text{em}}$ , whereas the oxidized nanoparticles exhibited a small blue shift (ca. 3 nm) of both  $\lambda_{\text{ex}}$  and  $\lambda_{\text{em}}$ . This observation is consistent with the results presented above (Figure 1 and 2), which suggests that reduction (oxidation) of the nanoparticles lead to enhanced (decreased) intraparticle charge delocalization. Although at this point it is not clear why a (slight) red shift of

both  $\lambda_{\text{ex}}$  and  $\lambda_{\text{em}}$  for the reduced nanoparticles was not observed, the reduced (oxidized) nanoparticles did exhibit a marked enhancement (diminishment) of the emission intensity. In fact, the ratio of the emission peak intensity of the three nanoparticles can be estimated to be Ru-OC<sub>Ox</sub>/Ru-OC/Ru-OC<sub>Red</sub> = 0.68:1:1.49 (note the optical absorbances of all three nanoparticles at  $\lambda_{\text{ex}}$  are almost the same; Figure 3, inset and Table 1), suggesting that the emission efficiency might be enhanced (decreased) by an increase (decrease) of the intraparticle charge delocalization. Similar behaviors were observed with pyrene-functionalized ruthenium nanoparticles having ruthenium–carbene  $\pi$  bonds;<sup>[7,8]</sup> the emission efficiency of the nanoparticle-bound pyrene moieties also decreased in the order reduced > as-prepared > oxidized nanoparticles (Supporting Information, Figures S3, S4). This observation is in agreement with earlier reports, where the quantum yield of  $\pi$ -conjugated molecules was found to be strongly dependent on the extent of conjugation.<sup>[25]</sup>

In summary, intraparticle charge delocalization of ruthenium nanoparticles passivated by 1-octynyl fragments was readily manipulated by the nanoparticle charge state, which was achieved by chemical reduction or oxidation. This is in sharp contrast to earlier work with gold nanoparticles passivated by thiol derivatives where the impacts of the depletion or injection of core free electrons were essentially confined to the metallic cores.<sup>[26]</sup> In the present study, electrochemical measurements suggested that the nanoparticles exhibited a net gain (loss) of 0.6 electron per particles by NaBH<sub>4</sub> reduction (Ce(SO<sub>4</sub>)<sub>2</sub> oxidation), leading to decreased (enhanced) bonding order of the particle-bound C≡C moieties, as manifested in FTIR and XPS measurements. The extended conjugation between the particle-bound C≡C moieties appear to be strengthened (weakened) when the nanoparticles were charged (discharged), which may be accounted for by the fact that the nanoparticle metallic cores serve as the conducting media to facilitate intraparticle charge delocalization. As a result, the nanoparticle photoluminescence characteristics vary accordingly. Whereas the peak position of the emission profiles only exhibits a slight variation, the intensity of the reduced nanoparticles was markedly enhanced, and that of the oxidized nanoparticles showed an apparent suppression relative to the as-prepared nanoparticles. These results demonstrate that the nanoparticle optoelectronic properties may be further manipulated by the nanoparticle charge state by taking advantage of the molecular capacitor characters of the particles and also the strong metal–ligand interfacial bonding interactions.

### Experimental Section

Ruthenium chloride (RuCl<sub>3</sub>, 99+%, ACROS), superhydride (LiB(C<sub>2</sub>H<sub>5</sub>)<sub>3</sub>H, 1M in THF, ACROS), 1-octyne (Alfa Aesar, 98%), *n*-butyllithium (*n*BuLi, ACROS), 1,2-propanediol (ACROS), sodium acetate trihydrate (NaOAc·3H<sub>2</sub>O, MC&B), sodium borohydride (NaBH<sub>4</sub>, 98%, ACROS), ceric sulfate (Ce(SO<sub>4</sub>)<sub>2</sub>, 99%, ACROS), and extra-dry *N,N*-dimethylformamide (DMF, 99.8%, Aldrich) were used as received. All solvents were obtained from typical commercial sources and used without further treatment. Water was supplied by a Barnstead Nanopure water system (18.3 MΩ cm).

<sup>1</sup>H NMR spectroscopic measurements were carried out by using concentrated solutions of the nanoparticles in CDCl<sub>3</sub> or CD<sub>2</sub>Cl<sub>2</sub> with a Varian Unity 500 MHz NMR spectrometer. UV/Vis spectroscopic studies were performed with an ATI Unicam UV4 spectrometer using a 1 cm quartz cuvette with a resolution of 2 nm. Photoluminescence characteristics were examined with a PTI fluorospectrometer. FTIR measurements were carried out with a Perkin–Elmer FTIR spectrometer (Spectrum One, spectral resolution 4 cm<sup>-1</sup>); the samples were prepared by casting the particle solutions onto a NaCl disk. X-ray photoelectron spectra (XPS) were recorded with a PHI 5400/XPS instrument equipped with an Al<sub>Kα</sub> source operated at 350 W and at 10<sup>-9</sup> Torr. Silicon wafers were sputtered by Argon ions to remove carbon from the background and used as substrates. The spectra were charge-referenced to the Au4f<sub>7/2</sub> peak (83.8 eV) of sputtered gold.

Received: August 9, 2010

Published online: October 28, 2010

**Keywords:** alkynes · charge delocalization · nanoparticles · ruthenium · XPS

- [1] M. Brust, M. Walker, D. Bethell, D. J. Schiffrin, R. Whyman, *J. Chem. Soc. Chem. Commun.* **1994**, 801.
- [2] R. L. Whetten, M. N. Shafiqullin, J. T. Khoury, T. G. Schaaff, I. Vezmar, M. M. Alvarez, A. Wilkinson, *Acc. Chem. Res.* **1999**, *32*, 397.
- [3] A. C. Templeton, M. P. Wuelfing, R. W. Murray, *Acc. Chem. Res.* **2000**, *33*, 27.
- [4] R. Shenhar, V. M. Rotello, *Acc. Chem. Res.* **2003**, *36*, 549.
- [5] W. Chen, S. W. Chen, F. Z. Ding, H. B. Wang, L. E. Brown, J. P. Konopelski, *J. Am. Chem. Soc.* **2008**, *130*, 12156.
- [6] W. Chen, L. E. Brown, J. P. Konopelski, S. W. Chen, *Chem. Phys. Lett.* **2009**, *471*, 283.
- [7] W. Chen, N. B. Zuckerman, J. W. Lewis, J. P. Konopelski, S. W. Chen, *J. Phys. Chem. C* **2009**, *113*, 16988.
- [8] W. Chen, N. B. Zuckerman, J. P. Konopelski, S. W. Chen, *Anal. Chem.* **2010**, *82*, 461.
- [9] W. Chen, N. B. Zuckerman, X. W. Kang, D. Ghosh, J. P. Konopelski, S. W. Chen, *J. Phys. Chem. C* **2010**, *114*, 18146.
- [10] J. J. Pietron, J. F. Hicks, R. W. Murray, *J. Am. Chem. Soc.* **1999**, *121*, 5565.
- [11] S. W. Chen, R. W. Murray, S. W. Feldberg, *J. Phys. Chem. B* **1998**, *102*, 9898.
- [12] D. R. Lide, *CRC Handbook of Chemistry and Physics, electronic ed.*, CRC Press, Boca Raton, **2001**.
- [13] F. P. Pruchnik, *Organometallic chemistry of the transition elements*, Plenum Press, New York, **1990**.
- [14] M. Tsutsui, A. Courtney, *Adv. Organomet. Chem.* **1977**, *16*, 241.
- [15] The structural integrity of the nanoparticles after reduction or oxidation was examined by FTIR and <sup>1</sup>H NMR measurements. The nanoparticle cores were decomposed by dilute KCN and the organic components were then extracted for spectroscopic analysis. FTIR measurements showed that the C≡C stretching mode from the three nanoparticle samples all emerged at 2100 cm<sup>-1</sup>, consistent with that observed with monomeric 1-octyne (Ref. [9]). Samples from the three nanoparticles also exhibited similar <sup>1</sup>H NMR features, with three major peaks appearing at 0.9 ppm, 1.2–1.4 ppm, and 1.8 ppm, which are assigned to the protons of CH<sub>3</sub>, CH<sub>2</sub>, and ≡CH, respectively; these values are again consistent with the molecular structure of 1-octyne (Ref. [9]).
- [16] A. Hu, M. Rybachuk, Q. B. Lu, W. W. Duley, *Appl. Phys. Lett.* **2007**, *91*, 131906.
- [17] M. Rybachuk, J. M. Bell, *Carbon* **2009**, *47*, 2481.
- [18] G. Iucci, V. Carravetta, P. Altamura, M. V. Russo, G. Paolucci, A. Goldoni, G. Polzonetti, *Chem. Phys.* **2004**, *302*, 43.
- [19] S. Turgeon, R. W. Paynter, *Thin Solid Films* **2001**, *394*, 43.
- [20] U. Dettlaff-Weglikowska, J. M. Benoit, P. W. Chiu, R. Graupner, S. Lebedkin, S. Roth, *Curr. Appl. Phys.* **2002**, *2*, 497.
- [21] K. Siegbahn, *Philos. Trans. R. Soc. London Ser. A* **1970**, 268, 33.
- [22] D. Briggs, J. T. Grant, *Surface Analysis by Auger and X-ray Photoelectron Spectroscopy*, IM Publications, Chichester, **2003**.
- [23] N. Chakroune, G. Viau, S. Ammar, L. Poul, D. Veautier, M. M. Chehimi, C. Mangeney, F. Villain, F. Fievet, *Langmuir* **2005**, *21*, 6788.
- [24] R. Luque, J. H. Clark, K. Yoshida, P. L. Gai, *Chem. Commun.* **2009**, 5305.
- [25] Y. Yamaguchi, Y. Matsubara, T. Ochi, T. Wakamiya, Z. I. Yoshida, *J. Am. Chem. Soc.* **2008**, *130*, 13867.
- [26] A. C. Templeton, J. J. Pietron, R. W. Murray, P. Mulvaney, *J. Phys. Chem. B* **2000**, *104*, 564.